The Astrophysical Journal, 925:149 (7pp), 2022 February 1 https://doi.org/10.3847/1538-4357/ac3de3

Energy Extraction via Magnetic Reconnection in the Ergosphere of a Rotating Non-Kerr Black Hole

Wenshuai Liu
Department of Astronomy, School of Physics, Huazhong University of Science and Technology, Wuhan 430074, People's Republic of China; 674602871@qq.com
Received 2021 September 28; revised 2021 November 25; accepted 2021 November 26; published 2022 February 2

Abstract

Magnetic reconnection in the ergosphere is investigated for a relativistic plasma around a rotating non-Kerr black hole. For a rotating non-Kerr black hole immersed in a magnetic field generated by an externally material, antiparallel magnetic field line could form in the ergosphere due to frame dragging. Therefore, magnetic reconnection could occur in the ergosphere. This magnetic reconnection may generate negative energy at infinity by redistributing the angular momentum during the process. The results show that, taking into account the effect of the deformed parameter, extraction of energy from a rotating non-Kerr black hole by magnetic reconnection could be enhanced in the presence of a positive deformed parameter.

Unified Astronomy Thesaurus concepts: Black hole physics (159); Plasma astrophysics (1261); Magnetic fields (994)

1. Introduction

According to the no-hair theorem (Israel 1968, 1972; Carter 1971; Hawking 1972; Robinson 1975), a rotating black hole with no electric charge is fully described by the Kerr metric with the mass of the black hole M and the dimensionless spin parameter a in asymptotically flat and matter-free spacetime. However, general relativity may break down in the case of strong gravity, meaning that the Kerr metric might not be the unique spacetime accounting for rotating black holes (Caravelli & Modesto 2010; Bambi & Modesto 2011; Johannsen & Psaltis 2011a). With this motivation, a deformed Kerr-like metric is proposed by Johannsen and Psaltis (2011a) that is suitable to describe a rotating non-Kerr black hole in the regime of strong gravity. The non-Kerr metric contains a deformed parameter ϵ which represents deviations from the Kerr metric.

Rotating black holes store rotational energy that can be extracted (Meier et al. 2001). Extraction of energy from a rotating black hole can produce significant energy outflows which are believed to account for some kinds of high-energy astrophysical processes, such as relativistic jets powered by black holes hosted in active galactic nuclei, gamma-ray bursts, and microquasars (Misner et al. 1970). Various processes of extracting energy from rotating black holes have been developed. Mechanisms accounting for energy extraction of rotating black holes include the Penrose process, superradiant scattering, Blandford–Znajek mechanism, magnetohydrodynamic Penrose process, and modified Hawking process (Penrose 1969; Press & Teukolsky 1972; Ruffini & Wilson 1975; Blandford & Znajek 1977; Hirotani et al. 1992; van Putten 1999). In particular, these different kinds of mechanisms of energy extraction are based on the idea of the Penrose process that it redistributes energy and angular momentum of which the negative part swallowed by the black hole will reduce the black hole mass. Recently, magnetic reconnection in the ergosphere of a Kerr black hole (Koide & Arai 2008; Comisso & Asenjo 2021) has been shown to be an efficient way of extracting energy from a Kerr black hole by producing a pair of outflows with equal velocity but opposite directions through redistributing the angular momentum of the plasma in a localized diffusion region, with some of the negative energy at infinity and the rest of the energy, which is larger than its rest mass and thermal energies, acting in the same way as in the Penrose process.

Energy extraction of rotating black holes as described above is proposed in the regime of the Kerr metric. Energy extraction by the Penrose process in the ergosphere of a rotating non-Kerr back hole was investigated by Liu et al. (2012) where they showed that the deformed parameter ϵ in the non-Kerr metric could play a significant role on the maximum efficiency of energy extraction due to the Penrose process, and could cause the efficiency to exceed to 60% compared with ∼20.7% in the ergosphere of the Kerr metric. In this work, we investigate in detail energy extraction via magnetic reconnection in the equatorial plane in the ergosphere of a rotating non-Kerr black hole and how the deformed parameter ϵ affects the efficiency of the energy extraction due to magnetic reconnection.

This work is organized as follows: in Section 2 we briefly describe the non-Kerr metric proposed by Johannsen and Psaltis and the physical background with which to study energy extraction due to magnetic reconnection in the ergosphere of a rotating non-Kerr black hole. We investigate the efficiency of the energy extraction via magnetic reconnection in Section 3. A discussion is given in Section 4 and a summary in Section 5. Throughout this work, we set the gravitational constant $G = 1$, mass of the non-Kerr black hole $M = 1$, and the speed of light $c = 1$.

2. Physical Background of Magnetic Reconnection in the Non-Kerr Spacetime

As with extraction of energy from a Kerr black hole in the ergosphere, that from a rotating non-Kerr black hole through the negative-energy particles swallowed by the black hole via magnetic reconnection in the ergosphere needs the condition that it occur in the ergosphere due to the fact that

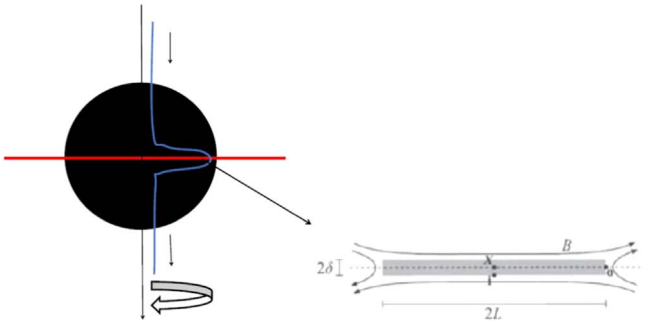

Figure 1. Magnetic configuration of magnetic reconnection in a black hole ergosphere. The red line represents the equatorial plane of the non-Kerr black hole. The blue curve, which is behind the black hole, shows the magnetic field line affected by the frame-dragging effect.

negative-energy orbits only exist in this region. Configuration of the antiparallel magnetic field lines with which magnetic reconnection could take place is a natural result of the frame-dragging effect as shown in Figure 1. Before investigating magnetic reconnection in the ergosphere of a rotating non-Kerr black hole, we first describe the physical background with which to study energy extraction via magnetic reconnection in the ergosphere.

The deformed Kerr-like metric around a rotating non-Kerr black hole in Boyer–Lindquist coordinates (t, r, θ, ϕ) can be expressed as (Johannsen & Psaltis 2011a)

$$ds^2 = g_{\rm tt}dt^2 + g_{\rm rr}dr^2 + g_{\theta\theta}d\theta^2 + g_{\phi\phi}d\phi^2 + 2g_{t\phi}dt\,d\phi, \quad (1)$$

with

$$\begin{aligned} g_{\rm tt} &= -\left(1 - \frac{2Mr}{\rho^2}\right)(1+h),\ g_{t\phi} = -\frac{2aMr\sin^2\theta}{\rho^2}(1+h), \\ g_{\rm rr} &= \frac{\rho^2(1+h)}{\Delta + a^2 h\sin^2\theta}, \qquad g_{\theta\theta} = \rho^2, \\ g_{\phi\phi} &= \sin^2\theta\left[\rho^2 + \frac{a^2(\rho^2+2Mr)\sin^2\theta}{\rho^2}(1+h)\right], \end{aligned} \quad (2)$$

where

$$\begin{aligned} \rho^2 &= r^2 + a^2\cos^2\theta,\ \Delta = r^2 - 2Mr + a^2, \\ h &= \frac{\epsilon M^3 r}{\rho^4}, \end{aligned} \quad (3)$$

and r, θ, ϕ represent the radial distance, the polar angle, and the azimuthal angle, respectively.

The constant ϵ represents the deformation parameter. ϵ with positive or negative value corresponds to the cases in which the compact object is more prolate or oblate than the Kerr black hole whose ϵ is equal to zero.

Energy extraction can happen in the ergosphere region of which is bounded by the event horizon r_H and the outer infinite redshift surface r_∞. The horizon of the black hole r_H is given by the maximum root of the following equation (Johannsen & Psaltis 2011a)

$$\Delta + a^2 h\sin^2\theta = 0 \quad (4)$$

and the outer infinite redshift surface is described by Liu et al. (2012)

$$r_\infty = M + (M^2 - a^2\cos^2\theta)^{\frac{1}{2}}, \quad (5)$$

which is the root of

$$1 - \frac{2Mr}{\rho^2} = 0. \quad (6)$$

Due to the presence of ϵ, the non-Kerr black hole could have an ergosphere only when (Liu et al. 2012)

$$-4(M + \sqrt{M^2 - a^2\cos^2\theta}) \leqslant \epsilon \leqslant \frac{\Delta\rho^4}{M^3 a^2 r\sin^2\theta}\Big|_{r=r_{tp}}, \quad (7)$$

where r_{tp} is the maximum positive root of (Liu et al. 2012)

$$\begin{aligned} &10r^4 - 16Mr^3 + a^2(7+\cos(2\theta))r^2 \\ &- a^4(1+\cos(2\theta)) = 0. \end{aligned} \quad (8)$$

In what follows, we study energy extraction using the 3+1 formalism, which has the advantage that it can isolate the effects of rotation of the spacetime, and is suitable to study plasmas surrounding rotating compact objects. In order to study the process of magnetic reconnection in the ergosphere of the rotating non-Kerr black hole analytically, we adopt a locally non-rotating frame called the zero angular momentum observer (ZAMO) frame (Bardeen et al. 1972) for convenience. Then we have the line element

$$ds^2 = -d\hat{t}^2 + \sum_i (d\hat{x}^i)^2 = \eta_{\mu\nu}d\hat{x}^\mu d\hat{x}^\nu \quad (9)$$

where $d\hat{t} = \alpha dt$, $d\hat{x}^i = h_i dx^i - \alpha\beta^i dt$, $\alpha = \sqrt{-g_{\rm tt} + \frac{g_{t\phi}^2}{g_{\phi\phi}}}$ and $\beta^\phi = -\frac{g_{t\phi}}{\alpha\sqrt{g_{\phi\phi}}}$.

Obviously, the spacetime is identical to Minkowski spacetime locally in the ZAMO frame. For a contravariant vector a^μ in the Boyer–Lindquist coordinates, $\hat{a}^\mu$ in the ZAMO frame is

$$\hat{a}^0 = \alpha a^0,\ \hat{a}^i = h_i a^i - \alpha\beta^i a^0 \quad (10)$$

and the covariant vector $\hat{a}_\mu$ is

$$\hat{a}_0 = \frac{1}{\alpha}a_0 + \sum_i \frac{\beta^i}{h_i}a_i,\ \hat{a}_i = \frac{1}{h_i}a_i. \quad (11)$$

Based on these transformations, we get the energy-at-infinity density $e^\infty = -\alpha g_{i0}T^{i0}$ with hatted variables observed in the ZAMO frame as follows (Koide & Arai 2008):

$$e^\infty = \alpha\hat{e} + \sum_i \omega_i h_i \hat{P}^i = \alpha\hat{e} + \alpha\beta^\phi\hat{P}^\phi \quad (12)$$

where $\hat{e}$ and $\hat{P}^\phi$ are the total energy density and the azimuthal component of the momentum density, respectively. They are given as (Koide & Arai 2008)

$$\hat{e} = \mathfrak{h}\hat{\gamma}^2 - p + \frac{\hat{B}^2 + \hat{E}^2}{2} \quad (13)$$

$$\hat{P}^\phi = \mathfrak{h}\hat{\gamma}^2\hat{v}^\phi + (\hat{\boldsymbol{E}}\times\hat{\boldsymbol{B}})^\phi \quad (14)$$

where $\mathfrak{h}$ is the enthalpy density.

In order to clearly show the energy-at-infinity density with hydrodynamic and electromagnetic components, Equation (12) can be separated as $e^\infty = e^\infty_{\rm hyd} + e^\infty_{\rm EM}$ where (Koide & Arai 2008)

$$e^{\infty}_{\rm hyd} = \alpha \hat{e}_{\rm hyd} + \alpha\beta^{\phi}\mathfrak{h}\hat{\gamma}^2\hat{v}^{\phi} \tag{15}$$

$$e^{\infty}_{\rm EM} = \alpha \hat{e}_{\rm EM} + \alpha\beta^{\phi}(\hat{\boldsymbol{E}} \times \hat{\boldsymbol{B}})^{\phi} \tag{16}$$

where $\hat{e}_{\rm hyd} = \mathfrak{h}\hat{\gamma}^2 - p$ and $\hat{e}_{\rm EM} = (\hat{B}^2 + \hat{E}^2)/2$ represent the hydrodynamic and electromagnetic energy densities observed in the ZAMO frame, respectively.

Here we consider the configuration of antiparallel magnetic field lines near the equatorial plane in the ergosphere resulting from frame dragging. For simplicity, we only investigate the hydrodynamic energy density at infinity with the assumption that magnetic reconnection converts most of the magnetic energy into plasma particle energy (Comisso & Asenjo 2021). Thus, the energy at infinity is mainly dominated by hydrodynamic energy. Therefore, Equation (15) becomes (Koide & Arai 2008)

$$e^{\infty}_{\rm hyd} = \alpha\left[\mathfrak{h}(\hat{\gamma} + \beta^{\phi}\hat{\gamma}\hat{v}^{\phi}) - \frac{p}{\hat{\gamma}}\right] \tag{17}$$

with the condition that the plasma is incompressible and adiabatic.

We assume the fluid element in the plasma corotates around the rotating non-Kerr black hole in the equatorial plane with Keplerian velocity, which can be expressed in Boyer–Lindquist coordinates (Bambi & Modesto 2011):

$$\Omega = \frac{d\phi}{dt} = \frac{-g_{t\phi,r} + \sqrt{g^2_{t\phi,r} - g_{tt,r}g_{\phi\phi,r}}}{g_{\phi\phi,r}}. \tag{18}$$

The above angular velocity can be written as a Keplerian velocity in the ϕ direction observed in the ZAMO frame, based on the transformation between a contravariant vector in the Boyer–Lindquist coordinates and that in the ZAMO frame:

$$\hat{v}_K = \frac{\Omega\sqrt{g_{\phi\phi}}}{\alpha} - \beta^{\phi}. \tag{19}$$

Circular orbits in the equatorial plane can exist from $r \to \infty$ to the circular photon orbit, which occurs at the radius at which (Johannsen & Psaltis 2011a)

$$\frac{E}{\mu} = \frac{1}{r^6}\sqrt{\frac{P_1 + P_2}{P_3}} \to \infty \tag{20}$$

and

$$\frac{L_z}{\mu} = \frac{1}{r^4 P_6\sqrt{P_3}}[\sqrt{M(r^3 + \epsilon_3 M^3)P_5} - 6aM(r^3 + \epsilon_3 M^3)\sqrt{P_1 + P_2}] \to \infty \tag{21}$$

where μ is the rest mass of a photon.

From Equations (20) and (21), we can get the radius where the circular photon orbit $r_{\rm ph}$ exists by solving $P_3 = 0$. However, circular orbits for a particle are stable only when $r > r_{\rm isco}$, where $r_{\rm isco}$ is the innermost stable circular orbit for non-spinning test particles, meaning that not all circular orbits are stable for $r > r_{\rm ph}$. For simplicity, we do not consider the stability of the circular orbit in this work.

In order to obtain the outflow velocity via the magnetic reconnection at small spatial scale, we introduce the local rest frame (t', $x^{1'}$, $x^{2'}$, $x^{3'}$) co-moving with the bulk plasma which rotates around the non-Kerr black hole in the circular orbit in the equatorial plane. The local rest frame is set with the condition that the direction of $x^{1'}$ is parallel to the direction r and the direction of $x^{3'}$ is parallel to the direction ϕ. The outflow velocity $v^{\phi'}$ and the outflow Lorentz factor γ' observed in the local rest frame can be changed to $\hat{v}^{\phi}$ and $\hat{\gamma}$ observed in the ZAMO frame through the following transformation (Takahashi 2007):

$$\hat{a}^{\mu} = e^{\mu}_{\nu'}a^{\nu'} \tag{22}$$

where

$$\begin{pmatrix} e^{\hat{t}}_{t'} & e^{\hat{t}}_{r'} & e^{\hat{t}}_{\theta'} & e^{\hat{t}}_{\phi'} \\ e^{\hat{r}}_{t'} & e^{\hat{r}}_{r'} & e^{\hat{r}}_{\theta'} & e^{\hat{r}}_{\phi'} \\ e^{\hat{\theta}}_{t'} & e^{\hat{\theta}}_{r'} & e^{\hat{\theta}}_{\theta'} & e^{\hat{\theta}}_{\phi'} \\ e^{\hat{\phi}}_{t'} & e^{\hat{\phi}}_{r'} & e^{\hat{\phi}}_{\theta'} & e^{\hat{\phi}}_{\phi'} \end{pmatrix} = \begin{pmatrix} \hat{\gamma} & \hat{\gamma}\hat{v}_r & 0 & \hat{\gamma}\hat{v}_{\phi} \\ \hat{\gamma}\hat{v}_r & 1 + \frac{\hat{\gamma}^2\hat{v}_r^2}{1+\hat{\gamma}} & 0 & \frac{\hat{\gamma}^2\hat{v}_r\hat{v}_{\phi}}{1+\hat{\gamma}} \\ 0 & 0 & 1 & 0 \\ \hat{\gamma}\hat{v}_{\phi} & \frac{\hat{\gamma}^2\hat{v}_r\hat{v}_{\phi}}{1+\hat{\gamma}} & 0 & 1 + \frac{\hat{\gamma}^2\hat{v}_{\phi}^2}{1+\hat{\gamma}} \end{pmatrix} \tag{23}$$

where $\hat{v}_r$ and $\hat{v}_{\phi}$ are the local rest frame's velocity in the radial and ϕ direction observed in ZAMO frame, respectively. In this work where the local rest frame co-moves with the bulk plasma rotating around the non-Kerr black hole in the circular orbit in the equatorial plane, it gives that $\hat{v}_r = 0$ and $\hat{v}_{\phi} = \hat{v}_K$.

We adopt the configuration of the reconnection layer in the azimuthal direction with the radially oriented current density; then we get the outflow velocity observed in the local rest frame as (Comisso & Asenjo 2021)

$$v_{\rm out} = \left(\frac{\sigma_0}{1 + \sigma_0}\right)^{\frac{1}{2}} \tag{24}$$

where $\sigma_0 = B_0^2/\mathfrak{h}_0$ is the plasma magnetization upstream of the reconnection layer, B_0 is the asymptotic macro-scale magnetic field, and $\mathfrak{h}_0$ is the enthalpy density (Comisso & Asenjo 2021).

With Equations (24) and (23), we get the outflow velocity observed in the ZAMO frame:

$$v^{\phi}_{\pm} = \frac{\hat{v}_K \pm v_{\rm out}}{1 \pm \hat{v}_K v_{\rm out}} \tag{25}$$

where $\pm$ represent the outflow velocity with corotating (+) and counterrotating (–) direction relative to the rotation of the non-Kerr black hole.

3. Extraction of Energy from a Non-Kerr Black Hole via Magnetic Reconnection

With Equations (25) and (17), we get the energy-at-infinity density of the reconnection outflows observed in the ZAMO frame as

$$e^{\infty}_{\rm hyd,\pm} = \alpha\hat{\gamma}_K\left[(1 + \hat{v}_K\beta^{\phi})\gamma_{\rm out}\mathfrak{h} \pm (\hat{v}_K + \beta^{\phi})\gamma_{\rm out}v_{\rm out}\mathfrak{h} - \frac{p}{(1 \pm \hat{v}_K v_{\rm out})\gamma_{\rm out}\hat{\gamma}_K^2}\right], \tag{26}$$

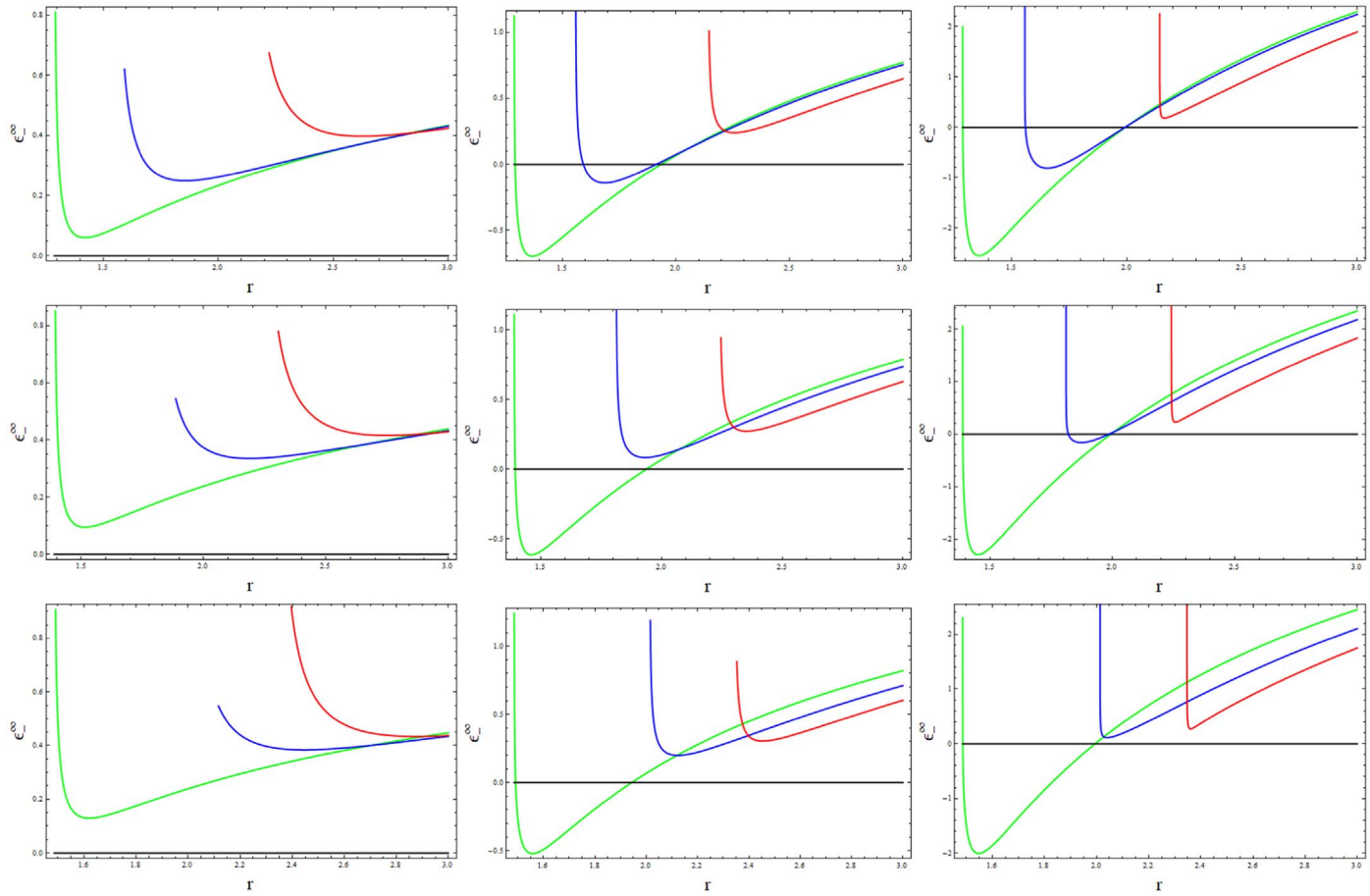

Figure 2. $\epsilon_{\pm}^{\infty}$ as a function of r with black hole spin $a = 0.9$ (top panels) $a = 0.8$ (middle panels), and $a = 0.7$ (bottom panels) and plasma magnetization $\sigma_0 = 1$, 10, 100 from left to right, respectively. Red and blue curves represent the results for $\epsilon = -1.8$ and $\epsilon = 0$, respectively. Green curves in the top, middle, and bottom panels represent the results for $\epsilon = 0.3$, $\epsilon = 0.9$, and $\epsilon = 1.9$, respectively.

where $\gamma_{\rm out} = (1 - v_{\rm out}^2)^{-\frac{1}{2}}$ and $\pm$ represent energy-at-infinity density of the accelerated $(+)$ outflow and decelerated $(-)$ outflow relative to the rotation of the black hole.

Then the hydrodynamic energy at infinity per enthalpy is (Comisso & Asenjo 2021)

$$\epsilon_{\pm}^{\infty} = \frac{e_{\rm hyd,\pm}^{\infty}}{\mathfrak{h}} = \alpha\hat{\gamma}_K\Bigg[(1 + \hat{v}_K\beta^{\phi})\gamma_{\rm out} \pm (\hat{v}_K + \beta^{\phi})\gamma_{\rm out}v_{\rm out} - \frac{1}{4(1 \pm \hat{v}_K v_{\rm out})\gamma_{\rm out}\hat{\gamma}_K^2}\Bigg], \tag{27}$$

where we set $\Gamma = \frac{4}{3}$.

With Equation (27), we can get the energy-at-infinity per enthalpy of the two outflows observed in the ZAMO frame after magnetic reconnection in the ergosphere of a rotating non-Kerr black hole. After magnetic reconnection, an interesting phenomenon is whether the energy-at-infinity of the decelerated outflow observed in the ZAMO frame can be negative or not. Since energy extraction through magnetic reconnection in the ergosphere of a Kerr black hole is studied in detail, here we focus on how the deformed parameter in the non-Kerr metric affects the energy of the decelerated outflow after magnetic reconnection in the ergosphere and the efficiency of the energy extraction.

In Figure 2 the energy-at-infinity of the decelerated plasma observed in the ZAMO frame is shown for different values of the deformed parameter ϵ, black hole spin a, and plasma magnetization σ_0. The parameter ϵ with posive/negative value is responsible for shifting $r_{\rm ph}$ toward/away from the central black hole, meaning that the minimum radius of circular orbit of plasma can decrease/increase when $\epsilon > 0/\epsilon < 0$. As seen from Figure 2, the radial region where energy extraction via magnetic reconnection can occur becomes large as ϵ increases for the same σ_0.

In Figure 3, the region of the phase-space $\{a, r\}$ where the rotational energy of a rotating non-Kerr black hole can be extracted by magnetic reconnection decreases as ϵ decreases for the same σ_0.

In order to illustrate the efficiency of energy extraction due to magnetic reconnection, we define (Comisso & Asenjo 2021)

$$\eta = \frac{\epsilon_{+}^{\infty}}{\epsilon_{+}^{\infty} + \epsilon_{-}^{\infty}} \tag{28}$$

as the efficiency of extraction of energy via magnetic reconnection. Energy extraction occurs when $\eta > 1$.

Figure 4 presents the efficiency η as a function of the radius for different ϵ, a, and σ_0. It shows that the efficiency increases as ϵ increases.

In real astrophysical systems hosting black holes, it is expected that the plasma magnetization in the ergosphere could be $\sigma_0 \geqslant 1$. In particular, in the case of supermassive black holes

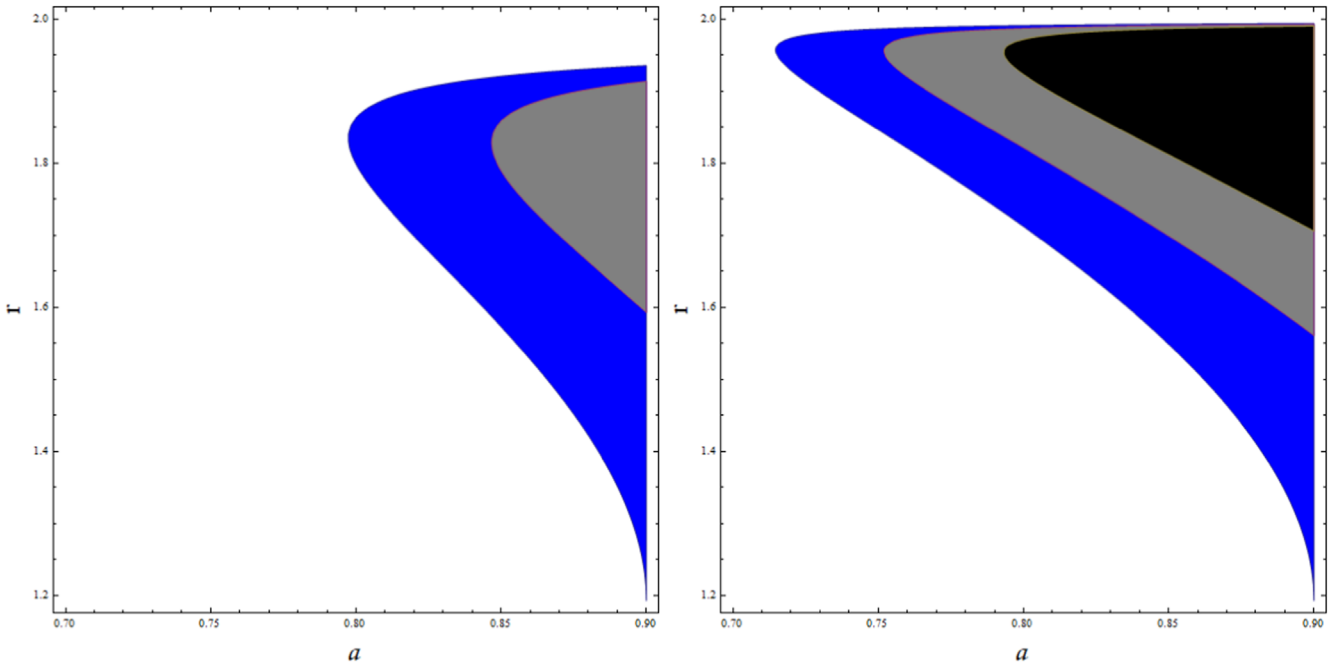

Figure 3. Regions of the phase-space $\{a, r\}$ where $\epsilon_{-}^{\infty} < 0$ with plasma magnetization $\sigma_0 = 10$ (left panel) and $\sigma_0 = 100$ (right panel). The blue, gray, and black regions represent the results for $\epsilon = 0.3202$, $\epsilon = 0$, and $\epsilon = -0.3$ respectively.

(SMBHs) in active galactic nuclei, the magnetization of plasma around such an SMBH could reach $\sigma_0 \sim 10^4$ or even larger (Dodds-Eden et al. 2010; Akiyama et al. 2019, 2021; Ponti et al. 2017). For the case of a stellar mass black hole governing gamma-ray bursts, the plasma magnetization in the ergosphere could be $\sigma_0 \sim 1$ or larger (MacFadyen & Woosley 1999; van Putten 1999; Kiuchi et al. 2015; Ruiz et al. 2019). With a high degree of plasma magnetization around a rotating non-Kerr black hole, efficient energy extraction of non-Kerr black holes via magnetic reconnection in the ergosphere could occur. This shows that the spin of the SMBH in M87 is about 0.9 (Tamburini et al. 2020); thus, it is expected that efficient extraction of energy via magnetic reconnection in the ergosphere of M87* could take place if the deformed parameter is positive compared with that with the Kerr metric. Many methods have been proposed to test the no-hair theorem in the strong-field regime (Barack & Cutler 2007; Apostolatos et al. 2009; Bambi & Freese 2009; Johannsen & Psaltis 2010, 2011b; Lukes-Gerakopoulos et al. 2010; Bambi & Barausse 2011; Bambi 2011, 2012a, 2012b, 2012c, 2013; Chen & Jing 2012a, 2012b; Krawczynski 2012). There is still a lack of accurate constraints on the deformed parameter of a given black hole based on current observations. From the theoretical point of view, magnetic reconnection in the ergosphere of a rotating non-Kerr black hole with large spin a, large plasma magnetization σ_0, and large, positive deformed parameter ϵ leads to extraction of energy with high efficiency.

4. Discussion

The SMBH in M87 shows bright TeV flares (Aharonian et al. 2006; Acciari et al. 2010; Aliu et al. 2012; Blanch 2021). It is conjectured that dissipation of magnetic energy resulting from magnetic reconnection is responsible for triggering flares powered by energetic electrons (Yuan et al. 2004; Broderick & Loeb 2005; Goodman & Uzdensky 2008; Younsi & Wu 2015; Ball et al. 2016; Li et al. 2017; Gutiérrez et al. 2020). Results from this work show that the deformed parameter can play a significant role on the outflow energy through magnetic reconnection in contrast with the Kerr spacetime. Plasmoids resulting from outflows produced by magnetic reconnection merge with other plasmoids, forming hot spots. Such hot spots filled with electrons energized by magnetic reconnection can power high-energy flares. Thus, features of the flares may be different between the non-Kerr and the Kerr spacetime with the same black hole spin and plasma magnetization, meaning that these features may be used to distinguish the non-Kerr from the Kerr black hole. Such features are based on magnetic reconnection simulations with general relativistic magnetohydrodynamics. This is beyond the scope of this work and we will undertake this in the future.

5. Summary

Energy extraction from a rotating non-Kerr black hole due to magnetic reconnection occurring in the ergosphere is investigated in this work. For a relativistic plasma rotating around a non-Kerr black hole, the magnetic field originating from the plasma can be affected by frame dragging, with the result that an antiparallel magnetic field line can form in the ergosphere near the equatorial plane. With this antiparallel magnetic field line configuration, a current sheet will form between the antiparallel magnetic field and is unstable in the presence of plasmoid instability. Magnetic reconnection will occur along with available magnetic energy converted into plasma particle energy as the current sheet is destroyed by the plasmoid instability and plasmoids/flux ropes form. Magnetic reconnection produces two components of outflows, with one accelerated in the direction of the rotation of the non-Kerr black hole and the other accelerated in the opposite direction. Energy extraction from a rotating non-Kerr black hole will occur when the energy-at-infinity of the outflow accelerated in the opposite direction from the non-Kerr black hole is negative and the outflow accelerated in the direction of the rotation of

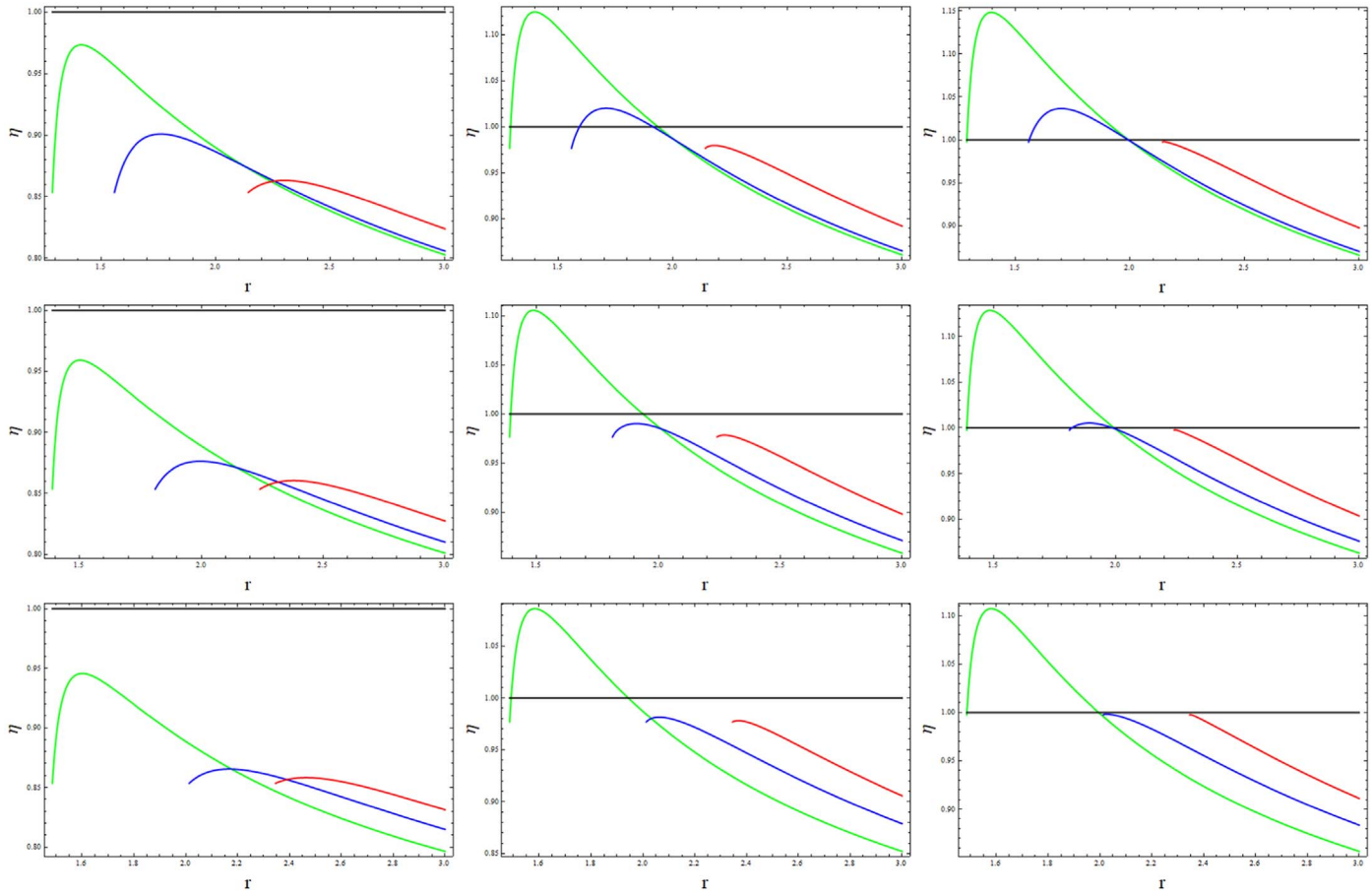

Figure 4. η as a function of r with black hole spin $a = 0.9$ (top panels) $a = 0.8$ (middle panels), and $a = 0.7$ (bottom panels) and plasma magnetization $\sigma_0 = 1$, 10, 100 from left to right, respectively. Red and blue curves represent the results for $\epsilon = -1.8$ and $\epsilon = 0$, respectively. Green curves in the top, middle, and bottom panels represent the results for $\epsilon = 0.3$, $\epsilon = 0.9$, and $\epsilon = 1.9$, respectively.

the black hole escapes to infinity after gaining energy from the black hole.

In this work, we focus our attention on the possibility of energy extraction by magnetic reconnection in the ergosphere of a rotating non-Kerr black hole. Our results show that the deformed parameter ϵ can strongly affect the energy state of the decelerated outflow via magnetic reconnection when compared with the standard Kerr metric. When the deformed parameter is positive, the radial region in the equatorial plane in the ergosphere where energy extraction by magnetic reconnection can occur becomes larger than that for the undeformed case while the opposite effect can emerge when the deformation is negative. The radial region where energy extraction via magnetic reconnection could occur is from $r = 1.2921$ to $r = 1.9346$ with $a = 0.9$, $\epsilon = 0.3$, and $\sigma_0 = 10$, which is larger than that from $r = 1.5927$ to 1.9138 with $a = 0.9$, $\epsilon = 0$, and $\sigma_0 = 10$ shown in the upper middle panel of Figure 2. In the upper right panel of Figure 2, the radial region from $r = 1.2883$ to $r = 1.9938$ with $a = 0.9$, $\epsilon = 0.3$, and $\sigma_0 = 100$ is larger than that from $r = 1.5607$ to $r = 1.9925$ with $a = 0.9$, $\epsilon = 0$, and $\sigma_0 = 100$. The middle right panel of Figure 2 shows that energy extraction can occur in the radial region from $r = 1.3899$ to $r = 1.9941$ with $a = 0.8$, $\epsilon = 0.9$, and $\sigma_0 = 100$; this region is larger than that from $r = 1.8211$ to 1.9869 with $a = 0.8$, $\epsilon = 0$, and $\sigma_0 = 100$. As shown in Figure 3, the region of phase-space $\{r, a\}$ where energy extraction via magnetic reconnection can occur increases as the deformed parameter increases for the same plasma magnetization. Compared with the Kerr black hole, the deformed parameter with positive value can enhance the efficiency of energy extraction via magnetic reconnection and the reduced efficiency occurs when the deformed parameter is negative; the region where the efficiency of energy extraction can be enhanced shown in Figure 4 is the same as that shown in Figure 2.

The reason why the radial region where energy extraction with a positive deformed parameter can occur is larger than that in the undeformed case is as follows. ϵ_{-}^{∞} from Equation (27) is found to be a monotonically decreasing function of ϵ when $r < 2$, meaning that ϵ_{-}^{∞} at a given radius (the radius is smaller than 2) decreases as ϵ increases for fixed σ_0 and a. With this feature of ϵ_{-}^{∞} and the fixed σ_0 and a, $\epsilon_{-}^{\infty} = 0$ with $\epsilon = 0$ has two roots, r_1 and r_2 ($r_2 > r_1$, $\epsilon_{-}^{\infty}(\epsilon = 0, r) < 0$ when $r_1 < r < r_2$), R_1 and R_2 ($R_2 > R_1$) are the roots of $\epsilon_{-}^{\infty} = 0$ with a given $\epsilon > 0$, and $\epsilon_{-}^{\infty}(\epsilon > 0, r) < 0$ when $R_1 < r < R_2$; we find that $\epsilon_{-}^{\infty}(\epsilon > 0, r_1) < \epsilon_{-}^{\infty}(\epsilon = 0, r_1) = 0$ and $\epsilon_{-}^{\infty}(\epsilon > 0, r_2) < \epsilon_{-}^{\infty}(\epsilon = 0, r_2) = 0$; thus, $R_1 < r_1$ and $R_2 > r_2$.

Magnetic reconnection in the vicinity of SMBH in M87 is thought to be the mechanism powering flares observed from M87*. Since the deformed parameter can strongly affect the outflow energy via magnetic reconnection in the ergosphere of a rotating non-Kerr black hole, distinctive features of the flares may emerge as a result of the presence of hot spots produced by the merger of plasmoids forming from outflows compared with that resulting from the Kerr spacetime, providing a possible method to distinguish the rotating non-Kerr black hole from the

Kerr one. Due to the fact that such features depend on general relativistic magnetohydrodynamic simulations which are beyond the scope of this paper, we will perform this work in the future.

I am very grateful to the anonymous referee for insightful comments that improved this work. This work is supported by the National Science Foundations of China (U1931203).

ORCID iDs

Wenshuai Liu https://orcid.org/0000-0002-5521-1425

References

Acciari, V. A., Aliu, E., Arlen, T., et al. 2010, ApJ, 716, 819
Aharonian, F., Akhperjanian, A. G., Bazer-Bachi, A. R., et al. 2006, Sci, 314, 1424
Akiyama, K., Alberdi, A., Alef, W., et al. 2019, ApJL, 875, L5
Akiyama, K., Algaba, J. C., Alberdi, A., et al. 2021, ApJL, 910, L13
Aliu, E., Arlen, T., Aune, T., et al. 2012, ApJ, 746, 141
Apostolatos, T. A., Lukes-Gerakopoulos, G., & Contopoulos, G. 2009, PhRvL, 103, 111101
Ball, D., Özel, F., Psaltis, D., & Chan, C. 2016, ApJ, 826, 77
Bambi, C. 2011, PhRvD, 83, 103003
Bambi, C. 2012a, PhRvD, 85, 043002
Bambi, C. 2012b, PhRvD, 86, 123013
Bambi, C. 2012c, ApJ, 761, 174
Bambi, C. 2013, PhRvD, 87, 023007
Bambi, C., & Barausse, E. 2011, ApJ, 731, 121
Bambi, C., & Freese, K. 2009, PhRvD, 79, 043002
Bambi, C., & Modesto, L. 2011, Phys. Lett. B, 706, 13
Barack, L., & Cutler, C. 2007, PhRvD, 75, 042003
Bardeen, J. M., Press, W. H., & Teukolsky, S. A. 1972, ApJ, 178, 347
Blanch, O. 2021, ATel, 14483, 1
Blandford, R. D., & Znajek, R. 1977, MNRAS, 179, 433
Broderick, A. E., & Loeb, A. 2005, MNRAS, 363, 353
Caravelli, F., & Modesto, L. 2010, CQGra, 27, 24502
Carter, B. 1971, PhRvL, 26, 331
Chen, S., & Jing, J. 2012a, Phys. Lett. B, 711, 81
Chen, S., & Jing, J. 2012b, PhRvD, 85, 124029
Comisso, L., & Asenjo, F. A. 2021, PhRvD, 103, 023014
Dodds-Eden, K., Sharma, P., Quataert, E., et al. 2010, ApJ, 725, 450
Goodman, J., & Uzdensky, D. 2008, ApJ, 688, 555
Gutiérrez, E. M., Nemmen, R., & Cafardo, F. 2020, ApJL, 891, L36
Hawking, S. W. 1972, Commun. Math. Phys., 25, 152
Hirotani, K., Takahashi, M., Nitta, S.-Y., & Tomimatsu, A. 1992, ApJ, 386, 455
Israel, W. 1968, Commun. Math. Phys., 8, 245
Israel, W. 1972, Phys. Rev., 164, 1776
Johannsen, T., & Psaltis, D. 2010, ApJ, 716, 187
Johannsen, T., & Psaltis, D. 2011a, PhRvD, 83, 124015
Johannsen, T., & Psaltis, D. 2011b, ApJ, 726, 11
Kiuchi, K., Sekiguchi, Y., Kyutoku, K., et al. 2015, PhRvD, 92, 064034
Koide, S., & Arai, K. 2008, ApJ, 682, 1124
Krawczynski, H. 2012, ApJ, 754, 133
Li, Y.-P., Yuan, F., & Wang, Q. D. 2017, MNRAS, 468, 2552
Liu, C., Chen, S., & Jing, J. 2012, ApJ, 751, 148
Lukes-Gerakopoulos, G., Apostolatos, T. A., & Contopoulos, G. 2010, PhRvD, 81, 124005
MacFadyen, A. I., & Woosley, S. E. 1999, ApJ, 524, 262
Meier, D. L., Koide, S., & Uchida, Y. 2001, Sci, 291, 84
Misner, C. W., Thorne, K. S., & Wheeler, J. A. 1970, Gravitation (San Francisco, CA: Freeman)
Penrose, R. 1969, Nuovo Cimento, 1, 252
Ponti, G., George, E., Scaringi, S., et al. 2017, MNRAS, 468, 2447
Press, W., & Teukolsky, S. A. 1972, Natur, 238, 211
Robinson, D. C. 1975, PhRvL, 34, 905
Ruffini, R., & Wilson, J. R. 1975, PhRvD, 12, 2959
Ruiz, M., Tsokaros, A., Paschalidis, V., & Shapiro, S. L. 2019, PhRvD, 99, 084032
Takahashi, R. 2007, MNRAS, 382, 567
Tamburini, F., Thide, B., & Della, V. M. 2020, MNRAS, 492, L22
van Putten, M. H. P. M. 1999, Sci, 284, 115
Younsi, Z., & Wu, K. 2015, MNRAS, 454, 3283
Yuan, F., Quataert, E., & Narayan, R. 2004, ApJ, 606, 894